Brazilian Journal of Chemical Engineering (2022) 39:55–66
https://doi.org/10.1007/s43153-021-00198-z

ORIGINAL PAPER

Study of the catalytic activity of multilayer graphene (MLG), molybdenum oxide (MoO_2), and manganese ferrite ($MnFe_2O_4$) on the melanoidin removal by ozonation process

Marcos Vinícius Mateus[1] · Mário Sérgio da Luz[1,2,3,4] · Rogério Valentim Gelamo[1,3] · Diego Andrade Lemos[2,3,4] · Cristiano Poleto[5] · Julio Cesar de Souza Inácio Gonçalves[1,2,3,4]

Received: 18 April 2021 / Revised: 18 November 2021 / Accepted: 19 November 2021 / Published online: 28 November 2021

Abstract

Melanoidin is a compound produced by food industries and distilleries, which has negative impacts on the water environment due to the high content of dissolved organic carbon and dark color. Consequently, this work aims to study the catalytic properties of multilayer graphene (MLG), molybdenum oxide (MoO_2), and manganese ferrite ($MnFe_2O_4$) in the ozonation process to remove melanoidin from water solution. The results show that the reaction rate constant (k) of the melanoidin decolorization process using catalytic ozonation is 1.7 times higher than the non-catalytic ozonation process. The same results were observed for all catalytic materials with no significant difference among them. On the other hand, MLG was the most efficient catalyst in removing total organic carbon. The removal efficiency was 32% for the non-catalytic ozonation process and 63% for the catalytic ozonation using MLG. This increase in efficiency is attributed to a better production of hydroxyl radicals in the presence of MLG, which was confirmed using isopropanol as a radical scavenger. The efficiencies using MoO_2 and $MnFe_2O_4$ were 46% and 51%, respectively. The results show that catalytic ozonation by MLG is a promising treatment for melanoidin removal.

Keywords Melanoidins · Catalytic materials · Multilayer graphene · Ozone · Ferrite

✉ Mário Sérgio da Luz
mario.luz@uftm.edu.br

1 Programa de Pós-Graduação Multicêntrico em Química, Universidade Federal do Triângulo Mineiro (UFTM), Avenida Dr. Randolfo Borges Júnior, n° 1400, Uberaba, MG CEP 38064-200, Brazil

2 Programa de Pós-Graduação em Ciência e Tecnologia Ambiental, Universidade Federal do Triângulo Mineiro (UFTM), Avenida Dr. Randolfo Borges Júnior, n° 1400, Uberaba, MG CEP 38064-200, Brazil

3 Instituto de Ciências Exatas e Tecnológicas, Universidade Federal do Triângulo Mineiro (UFTM), Avenida Dr. Randolfo Borges Júnior, n° 1400, Uberaba, MG CEP 38064-200, Brazil

4 Departamento de Engenharia Ambiental, Universidade Federal do Triângulo Mineiro (UFTM), Avenida Dr. Randolfo Borges Júnior, n° 1400, Uberaba, MG CEP 38064-200, Brazil

5 Departamento de Hidromecânica e Hidrologia, Instituto de Pesquisas Hidráulicas, Universidade Federal do Rio Grande do Sul (UFRGS), Avenida Bento Gonçalves, n° 9500, Porto Alegre, RS CEP 91501-970, Brazil

Introduction

Melanoidins are recalcitrant organic pollutants commonly found in urban wastewater (Dwyer et al. 2009), as well as in different industrial effluents, especially those associated with coffee and sugarcane processing, being the main component for the dark color of these effluents (Satori and Kawase 2014; Cabrera-Díaz et al. 2016; Chandra et al. 2018). Melanoidins are present in different foods, such as coffee, honey and beer, as they are a product of the Maillard reaction, a complex reaction that occurs during the heating of sugars and amino acids (Bruhns et al. 2019). The chemical properties of melanoidins are similar to those of humic substances; both being characterized as acidic, polymeric and highly dispersed colloids that present negative charge due to the dissociation of carboxylic and phenolic groups (Sachs and Bernhard 2011). However, an exact structure cannot be determined due to the wide variety of reaction paths and intermediates formed during the Maillard reaction (Mohsin et al. 2020; Ripper et al. 2020).

Due to their structural complexity and dark color, melanoidins pose a threat to the aquatic and terrestrial ecosystem (Chowdhary et al. 2018; Vivekanandam et al. 2019). The antioxidant and chelating properties of these compounds cause them to be toxic to many microorganisms associated with wastewater treatment and the aquatic environment (Kaushik et al. 2018; Ripper et al. 2020) and its dark colour compromises photosynthesis (Otieno and Apollo 2021). Some dyes, such as melanoidins, are resistant to conventional methods of biological treatment, whether aerobic or anaerobic, resulting in an incomplete color removal from wastewater (Li et al. 2017; Kaushik et al. 2018). During these processes, an increase in color may even occur due to the repolymerization of melanoidins (Peña et al. 2003; Mabuza et al. 2017). That said, the development of alternative technologies for the removal of melanoidins from urban wastewater is indispensable.

Recently, different approaches have been applied for the removal of melanoidins from wastewater, including membrane separation methods such as ultra and nanofiltration (Guo et al. 2019), reverse osmosis (Silva et al. 2019) and dialysis (Singh et al. 2018); and physical–chemical treatment methods such as coagulation/flocculation (Momeni et al. 2018), flotation/filtration (Christoforakos and Lazaridis 2018) and adsorption (Ahmed et al. 2020; Li et al. 2020; Rafigh and Soleymani 2020; Rizvi et al. 2020; Wongcharee and Aravinthan 2020). Alternative methods of biological treatment of melanoidins have emerged using, for example, microalgae (Tsioptsias et al. 2016), photosynthetic bacteria (Talaiekhozani and Rezania 2017), other specific bacteria (Chandra et al. 2018; Omar et al. 2020) and fungi (Kornilłowicz-Kowalska and Rybczyńska-Tkaczyk 2021), or even isolated enzymes (Zhang et al. 2019; Toomsan et al. 2020) and bio-electrochemical processes (Tsiakiri et al. 2020).

Both membrane separation methods and physical–chemical treatment methods showed excellent performance for color and organic load removal. However, these treatments may present limitations for large-scale application associated with accelerated membrane clogging, high reagent doses and costs, and high volumes of sludge generated (Romero et al. 2015; Thanapimmetha et al. 2017; Hoarau et al. 2018; Hollman et al. 2020). Although biological methods continue to gain strength in the field of wastewater treatment methods due to their inherent economic and ecological viability, these methods take longer to achieve the same efficiency in color and organic load removal (Chowdhary et al. 2018).

Advanced oxidative processes (AOPs) have attracted attention as highly competitive alternatives for the removal of dyes and other recalcitrant compounds (Nguyen et al. 2017; Alves et al. 2019; Araújo et al. 2020; Machado et al. 2020; Poblete et al. 2020; Tripathy et al. 2020; Raji et al. 2021). Ozone processes are AOPs of particular interest because they demonstrate ease of installation and operation, aptitude to remove turbidity, low influence on subsequent processes in the treatment plant and are able to synergize with other agents (other oxidants, catalysts and/or radiation) (Nawrocki 2013; Takashina et al. 2017; Setareh et al. 2020). It is especially worth highlighting the AOPs aptitude to increase the biodegradability of recalcitrant compounds such as melanoidins by direct or indirect attack (Aquino and Pires 2016). Chain reactions break these molecules into colorless aliphatic compounds and even mineralize them into simple products such as CO_2 and H_2O (Malik et al. 2019; Otieno et al. 2019). Thus, although AOPs generally have high costs, ozonation requires less energy and can be considered a cleaner solution, since it generates no secondary sludge (Romero et al. 2015; Malik et al. 2019).

However, the low transfer of ozone mass from the gas phase to the liquid phase and the resistance of some organic compounds to be degraded directly by ozone generally limit the efficiency of conventional ozonation technologies (Janknecht et al. 2001; Nawrocki 2013; Dias et al. 2020). By testing the limits of ozonation as tertiary treatment for secondary effluents of molasses fermentation industries, Fall et al. (2020) visualized a maximum reduction of 95% in color, but only 35% in chemical oxygen demand (COD). The introduction of catalysts can significantly increase the efficiency of the ozonation process due to increased generation of reactive oxygen species (ROS), such as hydroxyl radicals (·OH), superoxide radicals ($\cdot O_2^-$) and singlet oxygen ($^1O_2$) (Nawrocki and Kasprzyk-Hordern 2010; Biernacki et al. 2019; Wei et al. 2019). The nature of the generated ROS seems to depend on the type of catalyst used and some studies have even suggested that the dominant ROS have an influence on which pollutants will be targeted (Nawrocki 2013; Bing et al. 2015).

The results of Oliveira et al. (2019) indicated that the presence of $CoFe_2O_4$, as a magnetic catalyst, during synthetic melanoidin ozonation led to an increase from 75 to 98% in color removal and from 60 to 80% in total organic carbon (TOC) removal, attributed to the higher generation of ·OH. Metals, metal oxides and carbon-based materials have shown an excellent role as catalysts of the ozonation process (Gümüş and Akbal 2017; Ayoubi-Feiz et al. 2019; Afzal et al. 2019; Yuan et al. 2020). It was also demonstrated that the functional surface groups and structural properties (defect structures and textural properties) of a material highly influence its activity as catalyst (Liu et al. 2009; Cao et al. 2014; Xing et al. 2014). Innovative materials with unique structural properties such as graphene and graphene oxide are still poorly explored as catalysts in the ozonation process, having been used mainly as support for other materials that would act as catalysts (Wang et al. 2016; Zhang et al. 2018; Checa et al. 2019). Therefore, finding the

best catalyst for melanoidin ozonation is still an important demand to improve the treatment of urban wastewater.

In this context, this study aimed to evaluate the activity of three catalysts (i.e., multilayer graphene, MoO_2, $MnFe_2O_4$) in the ozonation process for degradation (TOC removal) and decolorization of melanoidin. It is important to note that these catalytic materials were chosen based on similar catalysts, previously used for removing melanoidin by the ozonation process (Arimi et al. 2015; Gümüş and Akbal 2017; Oliveira et al. 2019; Ayoubi-Feiz et al. 2019; Afzal et al. 2019; Yuan et al. 2020).

Materials and methods

Materials

D-Glucose ($C_6H_{12}O_6$) and glycine ($C_2H_5NO_2$) were purchased from Labsynth, Brazil. Sodium carbonate (Na_2CO_3), sodium sulfite (Na_2SO_3), and isopropyl alcohol (C_3H_8O) were purchased from Dinâmica, Brazil. Oxygen gas (99.5%) was supplied by IBG, Brazil. Molybdenum(IV) oxide (MoO_2, 99.99%) and manganese ferrite ($MnFe_2O_4$, 99.99%) were purchased from Sigma-Aldrich. The multilayer graphene (MLG) particles were obtained by thermal expansion of natural grafite donated by Nacional de Grafite Ltda, followed by mechanical exfoliation in organic solvent in an ultrasound bath, according to Machuno et al. (2015). MLG powder was obtained after organic solvent evaporation. All the reagents, which were of analytical grade, were used as received. The working solutions were prepared using deionized water.

Preparation of synthetic melanoidin

The synthetic melanoidin stock solution was prepared based on the methodology described by Kotsiopoulou et al. (2016). First, 4.5 g glucose, 1.88 g glycine and 0.42 g sodium bicarbonate were dissolved in 100 mL of deionized water under magnetic stirring. Then, the solution was heated in an oven for 7 h at 95 °C. After 7 h, the mixture was removed from the oven, and left to reach ambient temperature, then another 100 mL of deionized water were added (Liang et al. 2009).

Characterization of the catalysts

The morphology and chemical analysis of the catalysts were obtained with a scanning electron microscope (SEM) model LEO 1450VP with an Oxford energy dispersive spectrometer (EDS) and also using an atomic force microscope (AFM) by Agilent. Atomic force microscopy was used in order to investigate the MLG surface before and after the ozone experiment. A Shimadzu SPM9700 microscope was used together with a cantilever for dynamic mode purchased from NT MDT Co. The images were obtained using Gwyddion software (Nečas et al. 2012).

Ozonation experiments

Ozonation experiments were performed in a water-jacketed glass reactor (300 mL) at 25 °C. The temperature was maintained at the desired value by circulating water from a thermostatic bath (TECNAL TE-2005, Brazil) through a jacket surrounding the reactor. Ozone gas was generated from oxygen gas by an ozone generator (myOZONE M10, Brazil) at a concentration of 74 mg/L. The ozone was fed into the reactor through a porous silica diffuser at a flow rate of 1 L/min. The residual ozone in the off-gas from the reactor was absorbed by a 10% Na_2SO_3 aqueous solution. The schematic diagram of the reaction system is shown in Fig. 1.

The ozonation experiments were carried out in triplicate for each of the tested catalysts (MoO_2, $MnFe_2O_4$, and MLG) and without the presence of any catalysts at all (non-catalytic ozonation). Based upon Oliveira's et al. (2019) work, the reactor was filled with 250 mL of melanoidin aqueous solution (initial concentration = 300 mg/L; initial pH 6.9) and 0.1 g of catalyst, and posteriorly submitted to magnetic stirring (Fisatom 752A, Brazil) until the equilibrium adsorption was reached (30 min). The doses of catalysts were chosen based on previous work by Oliveira et al. (2019). Subsequently, ozone gas was fed into the reactor, and aliquots of the aqueous solution were collected at various time intervals (0, 60, 120 and 180 min) and filtered.

Color and organic carbon analyses

Color was analyzed using a UV–vis spectrophotometer (PerkinElmer Lambda25) at a maximum absorption wavelength of 475 nm, as suggested by Oliveira et al. (2019). A TOC analyzer (Shimadzu TOC-L CPH/CPN) was used for analyzing total organic carbon (TOC).

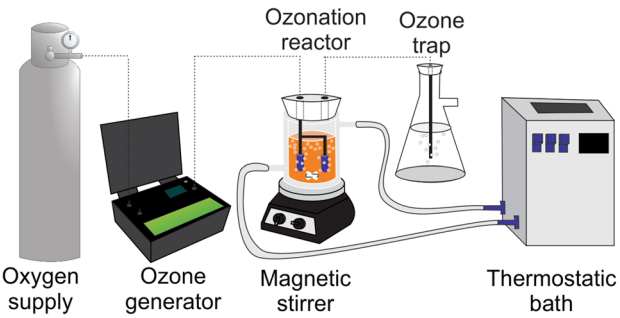

Fig. 1 Schematic representation of the ozonation system

Reusability of catalysts

The MLG catalyst was recovered after each ozonation experiment by Millipore vacuum filtration, washed with ultra-pure water and dried. Extra experiments were carried out to compensate the loss of catalyst during the recovery process. Catalytic activity was measured, using the recovered catalyst, and compared with the fresh catalyst.

Results and discussion

Characterization of catalyst materials

It is well known that the surface area and pore size of a catalyst material have huge impacts on the catalytic efficiency, as large surface area can provide more active sites where the reaction can occur (Gümüş and Akbal 2017; Bing et al. 2015; Chen et al. 2014; Bensetiti et al. 1997). Based on this, it is extremely important to know the microstructure of the materials used as catalysts.

The original microstructure of the catalyst powders is shown in Fig. 2 for multilayer graphene (MLG) (a), $MnFe_2O_4$ (b) and MoO_2 (c). From Fig. 2a it is possible to see that MLG is typically a platelet of thin layered structure with few graphene layers. The dispersion used herein consists of a diversity of particles with thickness ranging from 0.7 to 10 nm and area ranging from square nanometers to micrometers (about 1–5 μm^2). The $MnFe_2O_4$ and MoO_2 powders show similar morphology, which are composed of irregular particles with a high degree of agglomeration with average size of 10–20 µm. The agglomeration of $MnFe_2O_4$ can be attributed to the magnetic interactions between those particles (Li et al. 2009; Bakhteeva et al. 2015; Marimón-Bolívar and González 2018). The use of the EDS technique was important to evaluate the expected composition of all the catalyst powders, presented in Table 1.

Effect of reaction time on the color removal

Decolorization processes using ozone usually produce fast results, where time is not a significant variable. Corroborating this, the results of Fig. 3 show that the color of melanoidin solution was drastically reduced by almost 90% in just 10 min of reaction (with only ozone gas, see open circles). After 15 min, the impact of reaction time on color removal efficiency disappears and increasing the gas ozone dosage causes a significant increase in decolorization rates (not shown here). Peña et al. (2003) shows that ozonation of synthetic melanoidin under the same experimental conditions provided similar color removal efficiencies.

Despite the high efficiency using only ozone flowing in the solution, we decided to check if the presence of MoO_2,

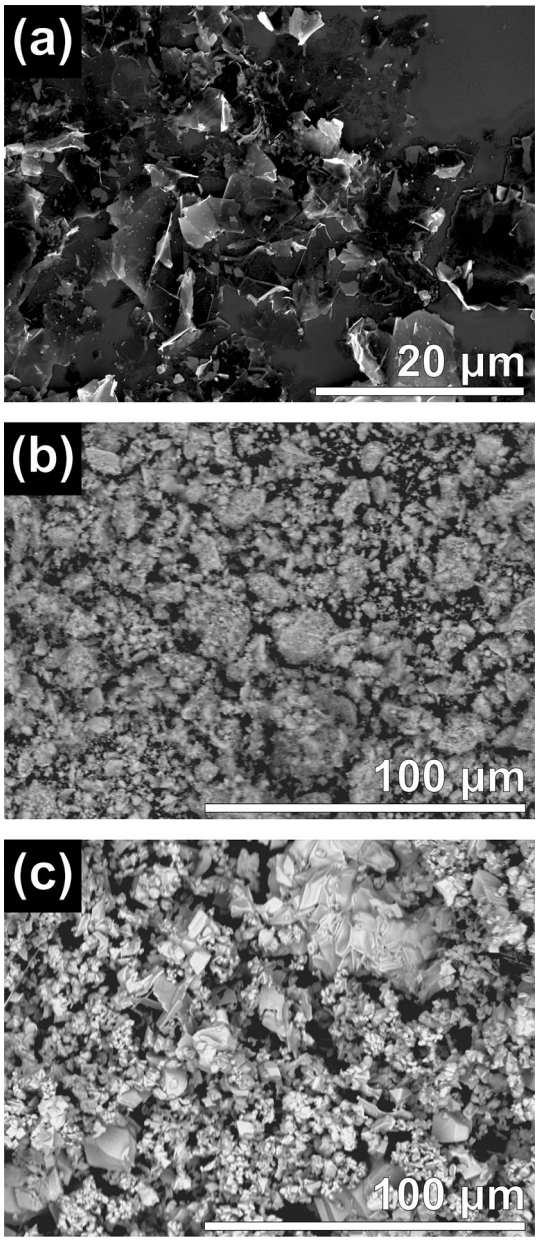

Fig. 2 SEM images of powders for **a** MLG, **b** $MnFe_2O_4$, and **c** MoO_2

Table 1 EDS elemental analysis for **a** MLG, **b** $MnFe_2O_4$, and **c** MoO_2 powders

	Element	Atomic %
(a)	Carbon	100.00
(b)	Oxygen	56.46
	Manganese	14.82
	Iron	28.72
(c)	Oxygen	69.30
	Molybdenum	30.70

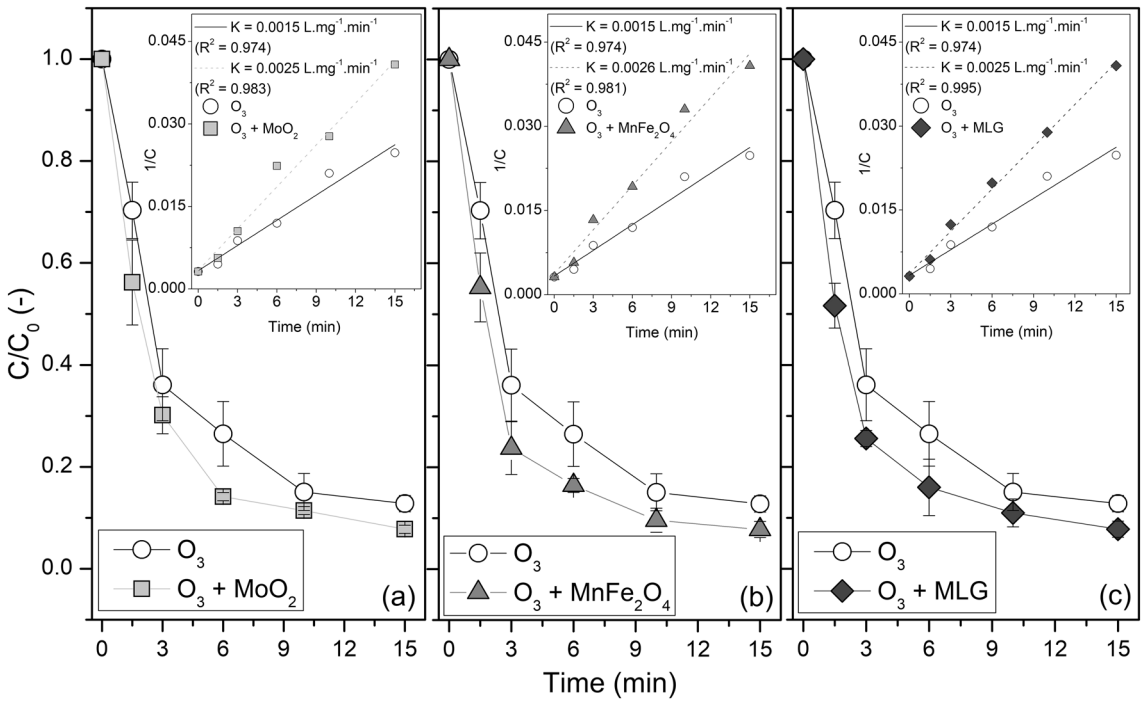

Fig. 3 Comparison of melanoidin decolorization by the non-catalytic system (with only ozone gas, see open circles) and catalytic ozonation processes using **a** MoO_2, **b** $MnFe_2O_4$, and **c** MLG, with ozone combined. The insets show the kinetics of melanoidin decolorization using non-catalytic and catalytic ozonation. The experiments were carried out in triplicate with O_3 at 1 L/min and 0.1 g catalysts (catalytic ozonation)

$MnFe_2O_4$ and MLG, with ozone combined, could interfere in the color removal process, at different reaction times. Those experimental results are also shown in Fig. 3. It is worth noting that the difference between the three catalytic powders was not significant and all of them showed similar behavior in terms of color removal. Compared to the results for non-catalytic ozonation, it can predict that the catalysts under investigation have a potential impact on the color removal in solutions containing melanoidin. To confirm this assumption, first and second order reaction kinetic models were considered to evaluate the kinetics of melanoidin decolorization in the presence of the three hetero-catalyst powders. The fitting results, presented in the inset of the Fig. 3, indicate that the decolorization reaction follows second order kinetics for all the catalytic systems. Similar analysis was reported for melanoidin decolorization of industrial effluent by natural manganese oxides (Arimi et al. 2015). For this order reaction, a R^2 greater than 0.974 for all experiments was found. In spite of this, an adjustment considering a first-order kinetic model showed a maximum R^2 of 0.884.

The reaction rate constants (k), for each system, could be calculated using the general pseudo-second order equation, as following:

$$\frac{1}{C} = \frac{1}{C_0} + kt, \tag{1}$$

where, t is the reaction time, C and C_0 are the concentrations of melanoidin at reaction time t and 0, respectively. The respective k were estimated by linear regression and are listed in the insets. We can observe that catalytic ozonation ($k = 0.0025$ L/mg/min for MoO_2 and MLG, and $k = 0.0026$ L/mg/min for $MnFe_2O_4$) was approximately 1.7 times higher than the non-catalytic ozonation reaction rate ($k = 0.0015$ L/mg/min). After 15 min, the efficiency of color removal was 87.2%, using the ozonation process, and 92.3% for all catalysts when using catalytic ozonation processes.

Figure 4 shows the color of melanoidin solutions during the ozonation reaction (without catalytic material). The first container (indicated as "0") corresponds to the raw solution, which has a brown color characteristic of the presence of melanoidin molecules. The solution decolorization increases as a function of reaction time so that, at the end of 15 min, a practically transparent solution was observed. The same apparent color behavior was observed in the catalytic ozonation processes.

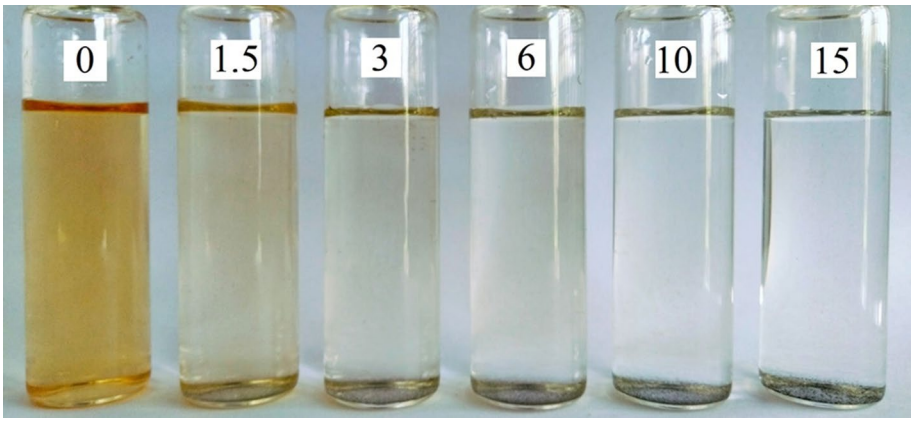

Fig. 4 Image of melanoidin solutions collected during the non-catalytic ozonation process for 0, 1.5, 3, 6, 10 and 15 min of reaction time

Total organic carbon (TOC) oxidation in melanoidin solutions

The most important parameter of wastewaters is color; however, this single parameter does not guarantee that the organic matter, present in these solutions, has been partially or completely mineralized (oxidized). Thus, total organic carbon (TOC) measurements were conducted to verify the effect of reaction time on catalytic oxidation capacity. Figure 5 shows the normalized TOC/TOC_0 (where TOC_0 is the total carbon organic estimated from the raw solution) in melanoidin solutions by ozonation (see open circles) and catalytic ozonation using MoO_2 (a), $MnFe_2O_4$ (b) and MLG (c), at different experimental times.

The results indicate that the content of total organic carbon in the solutions gradually decreased with catalyzed reaction time. The maximum removal rates of TOC at 180 min were 32%, 46%, 51% and 63%, using ozone alone, MoO_2, $MnFe_2O_4$ and MLG, respectively. Among these catalysts, MLG illustrated the highest removal efficiency. In addition, no adsorption of melanoidin was observed during 30 min prior to the reaction, with no ozone flowing into the system. In comparison, Oliveira et al. (2019) showed that, in similar conditions, catalytic ozonation of melanoidin in aqueous solution over catalyst showed about 80% removal of TOC at 180 min. In their work, $CoFe_2O_4$ showed a mesoporous structure with a large surface area, which can justify the greater efficiency of their catalyst.

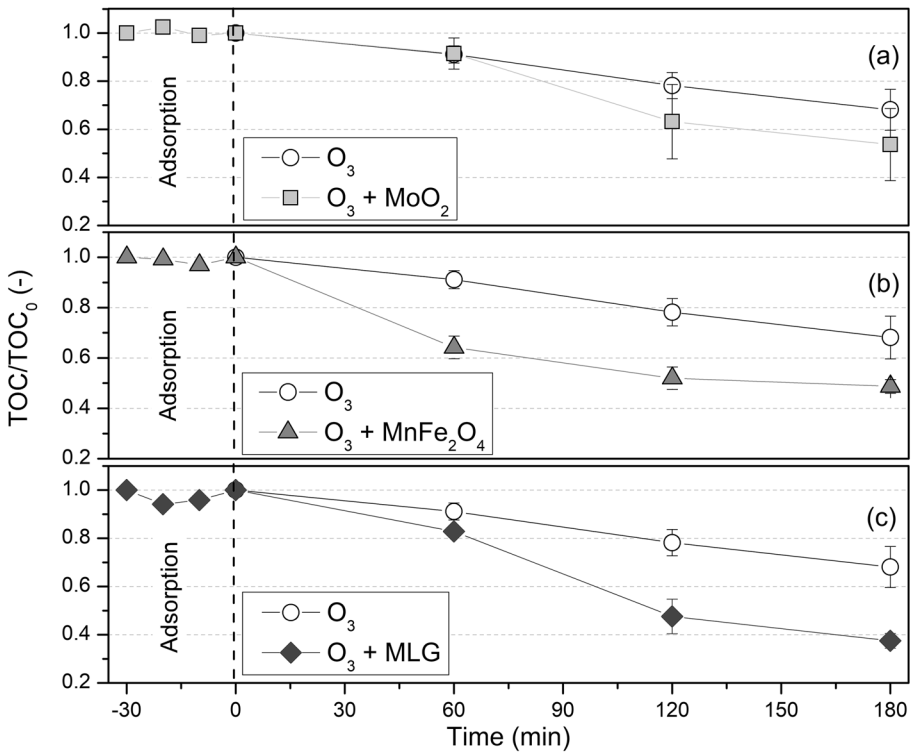

Fig. 5 Normalized TOC removal in melanoidin solutions by non-catalytic ozonation (open circles) and catalytic ozonation using **a** MoO_2, **b** $MnFe_2O_4$, and **c** MLG, at different experimental times (the lines connecting the experimental points are only a guide for eyes). The experiments were carried out in triplicate with O_3 at 1 L/min and 0.1 g catalysts (catalytic ozonation)

Figure 5 also shows that, when the catalytic oxidation time exceeded 180 min, the removal rates of TOC seem to saturate for all the catalytic systems. After that, macromolecular organics were degraded into small organic molecules, which could no longer be oxidized by ozonation and catalytic ozonation.

In addition, it is important to note that a further increase in the catalytic dosage did not show significant improvements in the degradation of organic matter, for all systems studied. This can be explained by the saturation of active sites due to the agglomeration of catalysts in the solution. In fact, powder agglomeration plays an important role in the efficiency of a catalyst, since accessibility to active sites decreases, with the consequent decrease in surface area in aggregate systems. (Bakhteeva et al. 2015; Marimón-Bolívar and González 2018). To reduce the agglomeration issue, different materials and treatments have been employed (Luciano et al. 2020; Baig et al. 2021; Zhu et al. 2020). However, the high cost involved in these catalytic processes is not welcome in wastewater treatment plants. However, even without reaching a complete organic matter oxidation, our results are promising and can serve as a basis for the development of more effective wastewater treatment systems, especially when using MLG as a catalyst. There is therefore a need to conduct intensive analysis of cost and compare it with other similar treatment methods.

Back to the catalytic ozonation results, ozone molecules dissolved in aqueous solution can be decomposed into ·OH and oxidize melanoidin, even without the presence of a catalyst material. On the other hand, MoO_2, $MnFe_2O_4$ and MLG powders significantly accelerated the ozonation process, improving the O_3 decomposition and consequently ·OH production. Several mechanisms for catalytic ozonation have been reported in the literature (Oliveira et al. 2019; Zhao et al. 2020). For MoO_2 and $MnFe_2O_4$, an interaction model has been assumed, previously reported in the literature (Oliveira et al. 2019), based on the following steps. In a first step, H_2O molecules are adsorbed and activated on the catalytic surface, where Mo and Mn ions serve as the active sites to transfer redox electrons to the deoxidizing agent. After that, ozone molecules are interconnected in the form of $MnFe_2O_4$-OH^--O_3 and MoO_2-OH^--O_3, forming activated species such as $\cdot O_2H$, $\cdot O_2^-$, as shown in the equations (Oliveira et al. 2019):

$$MnFe_2O_4\text{-}OH^- + O_3 \rightarrow \cdot O_2H + \cdot O_2^- + MnFe_2O_4, \quad (2)$$

$$MoO_2\text{-}OH^- + O_3 \rightarrow \cdot O_2H + \cdot O_2^- + MoO_2. \quad (3)$$

In the next steps, $\cdot O_2^-$ reacts with further O_3, producing $\cdot O_3^-$, which decomposes into ·OH species, according to Eqs. (4), (5) and (6):

$$\cdot O_2^- + O_3 \rightarrow O_2 + \cdot O_3^-, \quad (4)$$

$$\cdot O_3^- + H \rightarrow \cdot O_3H, \quad (5)$$

$$\cdot O_3H \rightarrow O_2 + \cdot OH. \quad (6)$$

An increase in the production of ·OH in the presence of MoO_2 and $MnFe_2O_4$ explains the increase in oxidized organic matter, compared to the ozonation process. When comparing both materials, $MnFe_2O_4$ is the most efficient catalyst. This can be attributed to the fact that Mn has superior electron transport properties than Mo, which can boost electron transfer accelerating the ozone decomposition process. $MnFe_2O_4$ can be easily recovered from the melanoidin solution, using an external magnetic field (Oliveira et al. 2019), and several authors have shown that $MnFe_2O_4$ can be reused as a catalyst in similar ozonation processes (Wang et al. 2018; Chen et al. 2014 and references therein). In addition, Bento et al. (2015) have reported the reusability of MoO_2 in olefin epoxidation catalytic experiments.

Now, let us discuss what happens during catalytic ozonation using MLG, which resulted in the greatest efficiency of removing organic matter among the catalytic ozonation processes. The mechanism involved follows the same above discussed processes for the other catalysts, in which hydroxyl radicals are responsible for degrading macromolecular melanoidin since the graphene structure presents a great ability to donate electrons to ozone, inducing reaction and decomposition. To confirm this, a set of experiments were conducted using isopropanol as scavenger to trap the generated ·OH. The same experiments shown in Fig. 5 were repeated for MLG in the presence, and absence, of isopropanol (see Fig. 6).

It is possible to observe that the TOC removal rate is reduced when the scavenger is added (O_3 + MLG + scavenger), becoming almost the same as for non-catalytic ozonation. This result indicates that ·OH is the oxidative species involved in the degradation of melanoidin using MLG as a catalyst.

Isopropanol reduces the TOC removal efficiency from 63 to 39%, indicating that the addition of isopropanol (scavenger) has no influence on the degradation of melanoidin in the non-catalytic ozonation process. With this information, it is possible to conclude that in the absence of MLG, mineralization occurs almost directly by O_3, while in the presence of the catalyst there is an expressive contribution from ·OH production. Oliveira et al. (2019) showed similar results, using $CoFe_2O_4$ as a heterogeneous catalyst. They report that, in the catalytic ozonation process, hydroxyl radicals are created with an oxidation potential of 2.80 eV, bigger than 2.07 eV for the ozonation process.

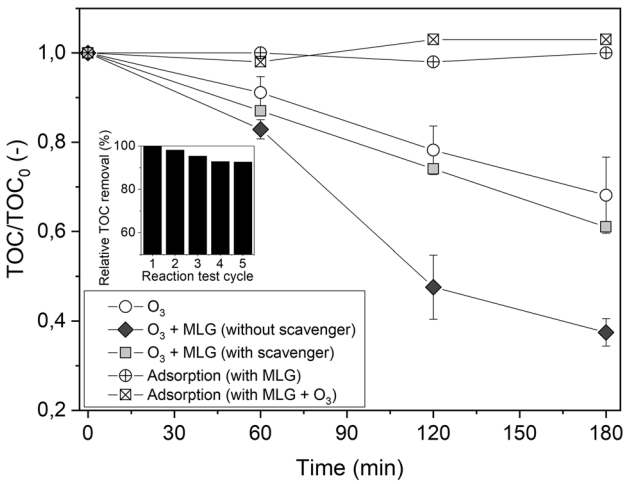

Fig. 6 Normalized TOC removal in melanoidin solutions by ozonation (open circles) and catalytic ozonation using MLG with (closed square) and without scavenger (closed diamond), at different experimental times. The figure also shows adsorption experiments carried out only with MLG (⊕) and with MLG + O_3 (⊠).The experiments were carried out in triplicate with O_3 at 1 L/min and 0.1 g catalysts (catalytic ozonation)

Figure 6 also shows that melanoidin molecules are not adsorbed by MLG. Adsorption experiments were performed during 180 min to show that oxidation is the only process for removing TOC during the ozonation and catalytic ozonation processes. The adsorption experiments were carried out under two different conditions: using raw MLG and ozone-treated MLG (the MLG powder was exposed to ozone for 180 min, in deionized water).

Additionally, the inset of Fig. 6 shows the reusability of MLG catalysts through five successive TOC measurements. The results show that MLG is reusable with relatively weak loss of catalytic activity. Percentage of relatively TOC removal decreased only 7%, comparing fresh MLG (taken as 100%), with the four-time reused catalyst. The loss of catalytic activity could be attributed to changes in the surface of MLG during the ozonation process. In fact, multilayer graphene (MLG) has excellent characteristics, such as high electrical and thermal conductivities (Natividade et al. 2019) and it is supposed to have a large surface area (Balandin 2011). It is also known that releasing similar materials, such as graphene and graphene oxide (GO), into water and wastewater treatment plants can cause physicochemical transformations in these materials, especially when ozone is flowing in the system (Tao et al. 2011; Yang et al. 2014; Du et al. 2019). For example, microscopie analyses showed that ozonation led to crumpling of GO nanosheets, truncation of GO edges, formation of holes, and production of small-sized graphenic fragments (Du et al. 2019). Figure 7 shows atomic force microscopy (AFM) images of an agglomeration of MLG pellets before and after the ozonation process. It can be observed that, after being exposed to ozone the MLG surface changes in appearance, especially in the graphene borders. After the ozone exposition, the border of the material has a more accentuated enhancement that may be associated with the oxidation of carbon atoms in this region, since breaking bonds in graphene edges is easier (Pereira et al. 2019). It is also possible to observe the presence of particulates of different sizes on the graphene surface, probably from MLG. So, we conclude that the ozonation process increases the concentration of defective sites in MLG, which highly influence the ·OH production leading to the greatest efficiency in removing organic matter among the other catalytic materials. In addition, the MLG has a huge surface area, which also positively assists in catalytic processes.

Conclusions

This work evaluated the effect of the catalysts MoO_2, $MnFe_2O_4$ and MLG on the ozonation process to decolorize and degrade melanoidin in water solution. To do this, a jacketed reactor (300 mL) was used where the solution was kept at 25 °C, and received ozone gas (flow rate = 1 L/min; concentration = 74 mg/L). The main conclusions are:

1. All catalytic materials improved the performance of the ozonation process for both color removal and TOC degradation in the melanoidin solution.
2. The performance among the catalysts was practically the same in terms of color removal.
3. Catalytic ozonation using MLG showed the best efficiency in removing TOC from the melanoidin solution after 180 min of reaction. The efficiency practically doubled when compared to non-catalytic ozonation.
4. The increase in TOC removal efficiency, using MLG, is attributed to the generation of more hydroxyl radicals in the presence of this catalyst.
5. MLG showed changes in its surface during the ozonation process. However, these changes apparently did not affect its functions as a catalyst in the ozonation process and also did not add other removal mechanisms to the process, such as adsorption.

Based on the above, it is concluded that catalytic ozonation is a promising process for removing melanoidin, which is currently found in industrial effluents. This work contributed to expand the options of catalysts that can be used to increase the efficiency of effluent treatment plants, indicating that MLG (a heterogeneous catalyst never before evaluated) has great potential for this purpose. Corroborating this, MGL is a metal-free material, mainly free of noble and transition metals, which are toxic and can pollute the environment.

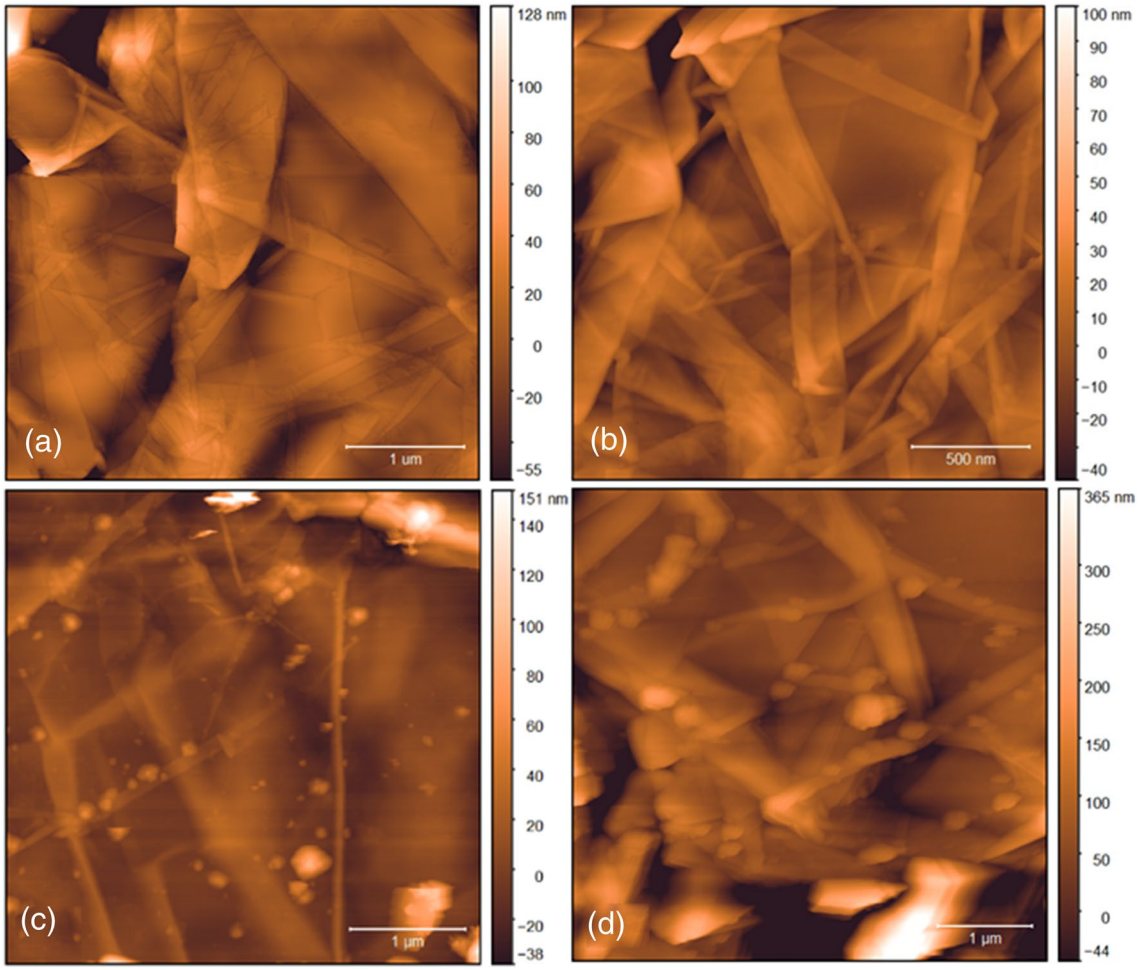

Fig. 7 Graphene morphology obtained by AFM for non-treated (**a**, **b**), after ozone treatment (**c**, **d**). The images were obtained using Gwyddion software (Nečas et al. 2012)

Finally, this work should improve the understanding of catalytic ozonation processes and promote their future application, especially for removal of emerging pollutants. It could assist in the development of new ozonation processes, especially for applications of graphene-based materials.

Acknowledgements This work is based upon financial support from the Fundação de Amparo à Pesquisa do Estado de Minas Gerais (FAPEMIG-APQ-02861-21), Conselho Nacional de Desenvolvimento Científico e Tecnológico (CNPq), and Coordenação de Aperfeiçoamento de Pessoal de Nível Superior (CAPES). The authors also thank Leandro for helping in the SEM/EDS experiments.

Declarations

Conflict of interest The authors certify that they have no affiliations with or involvement in any organization or entity with any financial interest in the subject matter or materials discussed in this manuscript.

References

Afzal S, Quan X, Lu S (2019) Catalytic performance and an insight into the mechanism of CeO_2 nanocrystals with different exposed facets in catalytic ozonation of *p*-nitrophenol. Appl Catal B Environ 248:526–537. https://doi.org/10.1016/j.apcatb.2019.02.010

Ahmed S, Unar IN, Khan HA, Maitlo G, Mahar RB, Jatoi AS, Shah AK (2020) Experimental study and dynamic simulation of melanoidin adsorption from distillery effluent. Environ Sci Pollut Res 27:9619–9636. https://doi.org/10.1007/s11356-019-07441-8

Alves PHL, Silva PSL, Ferreira DC, Gonçalves JCSI (2019) COD removal from sucrose solution using hydrodynamic cavitation and hydrogen peroxide: a comparison between Venturi device and orifice plate. Braz J Water Resourc. https://doi.org/10.1590/2318-0331.241920180147

Aquino S, Pires EC (2016) Assessment of ozone as a pretreatment to improve anaerobic digestion of vinasse. Braz J Chem Eng 33(2):279–285. https://doi.org/10.1590/0104-6632.20160332s20140141

Araujo MN, Soeira TVR, Poleto C, Rezende EGF, Cappa OAP, Ferreira DC, Rocha VC, Gonçalves JCSI (2020) Natural organic

matter degradation using hydrodynamic cavitation and hydrogen peroxide. Revista Eletrônica Em Gestão Educação e Tecnologia Ambiental. https://doi.org/10.5902/2236117062708

Arimi MM, Zhang Y, Götz G, Geißen SU (2015) Treatment of melanoidin wastewater by anaerobic digestion and coagulation. Environ Technol 36(19):2410–2418. https://doi.org/10.1080/09593330.2015.1032366

Ayoubi-Feiz B, Mashhadizadeh MH, Sheydaei M (2019) Degradation of diazinon by new hybrid nanocomposites N-TiO_2/graphene/Au and N-TiO_2/graphene/Ag using visible light photo-electro catalysis and photo-electro catalytic ozonation: optimization and comparative study by Taguchi method. Sep Purif Technol 2011:704–714. https://doi.org/10.1016/j.seppur.2018.10.032

Baig MM, Zulfiqar S, Yousuf MA, Shakir I, Aboud MFA, Warsi MF (2021) $Dy_xMnFe_{2-x}O_4$ nanoparticles decorated over mesoporous silica for environmental remediation applications. J Hazard Mater 402:123526. https://doi.org/10.1016/j.jhazmat.2020.123526

Bakhteeva I, Medvedeva I, Byzov I, Zhakov S, Yermakov A, Uimin M, Shchegoleva N (2015) Magnetic field-enhanced sedimentation of nanopowder magnetite in water flow. Environ Technol 36(13–16):1828–1836. https://doi.org/10.1080/09593330.2015.1013570

Balandin A (2011) Termal properties of graphene and nanostructured carbon materials. Nat Mater 10:569–581. https://doi.org/10.1038/nmat3064

Bensetiti Z, Schweich D, Abreu CAM (1997) The sensitivity of the catalyst effectiveness factor to pore size distribution. Braz J Chem Eng 14:4605. https://doi.org/10.1590/S0104-66321997000300013

Biernacki W, Fijołek L, Nawrocki J (2019) Dissolved ozone decomposition in presence of activated carbon at low pH: How experimental parameters affect observed kinetics of the process. Ozone Sci Eng. https://doi.org/10.1080/01919512.2018.1535889

Bing J, Hu C, Nie Y, Yang M, Qu J (2015) Mechanism of catalytic ozonation in Fe_2O_3/Al_2O_3@SBA-15 aqueous suspension for destruction of ibuprofen. Environ Sci Technol 49(3):1690–1697. https://doi.org/10.1021/es503729h

Bruhns P, Kanzler C, Degenhardt AG, Koch TJ, Kroh LW (2019) Basic structure of melanoidins formed in the Maillard reaction of 3-deoxyglucosone and γ-aminobutyric acid. J Agric Food Chem 67(18):5197–5203. https://doi.org/10.1021/acs.jafc.9b00202

Bento A, Sanches A, Medina E, Nunes CD, Vaz PD (2015) MoO2 nanoparticles as highly efficient olefin epoxidation catalysts. Applied Catalysis A: General 504:399–407. https://doi.org/10.1016/j.apcata.2015.03.024

Cabrera-Díaz A, Pereda-Reyes I, Dueñas-Moreno J, Véliz-Lorenzo E, Díaz-Marrero MA, Menéndez-Gutiérrez CL, Zaiat M (2016) Combined treatment of vinasse by an upflow anaerobic filter-reactor and ozonation process. Braz J Chem Eng 33(4):753–762. https://doi.org/10.1590/0104-6632.20160334s20150268

Cao H, Xing L, Wu G, Xie Y, Shi S, Zhang Y, Crittenden JC (2014) Promoting effect of nitration modification on activated carbon in the catalytic ozonation of oxalic acid. Appl Catal B 146:169–176. https://doi.org/10.1016/j.apcatb.2013.05.006

Chandra R, Kumar V, Tripathi S (2018) Evaluation of molasses-melanoidin decolourisation by potential bacterial consortium discharged in distillery effluent. 3 Biotech 8:187. https://doi.org/10.1007/s13205-018-1205-3

Checa M, Figueredo M, Aguinaco A, Beltrán FJ (2019) Graphene oxide/titania photocatalytic ozonation of primidone in a visible LED photoreactor. J Hazard Mater 369:70–78. https://doi.org/10.1016/j.jhazmat.2019.02.025

Chen J, Wen W, Kong L, Tian S, Ding F, Xiong Y (2014) Magnetically separable and durable $MnFe_2O_4$ for efficient catalytic ozonation of organic pollutants. Ind Eng Chem Res 53:6297–6306. https://doi.org/10.1021/ie403914r

Chowdhary P, Raj A, Bharagava RN (2018) Environmental pollution and health hazards from distillery wastewater and treatment approaches to combat the environmental threats: a review. Chemosphere 194:229–246. https://doi.org/10.1016/j.chemosphere.2017.11.163

Christoforakos NP, Lazaridis NK (2018) Melanoidin removal from aqueous systems by a hybrid flotation-filtration technique. J Chem Technol Biotechnol 93(8):2422–2428. https://doi.org/10.1002/jctb.5591

Dias NC, Alves TLM, Azevedo DA, Bassin JP, Dezotti M (2020) Metabolization of by-products formed by ozonation of the azo dye Reactive Red 239 in moving-bed biofilm reactors in series. Braz J Chem Eng. https://doi.org/10.1007/s43153-020-00046-6

Du T, Adeleye AS, Zhang T, Yang N, Hao R, Li Y, Chen W (2019) Effects of ozone and produced hydroxyl radical on the transformation of graphene oxide in aqueous media. Environ Sci Nano 6:2484–2494. https://doi.org/10.1039/c9en00361d

Dwyer J, Griffiths P, Lant P (2009) Simultaneous colour and DON removal from sewage treatment plant effluent: Alum coagulation of melanoidin. Water Res 43(2):553–561. https://doi.org/10.1016/j.watres.2008.10.053

Fall C, Barrón-Hernández LM, Olguín-Gutierrez MT, Bâ KM, Esparza-Soto M, Lucero-Chávez M (2020) Tertiary treatability of molasses secondary effluents for color and organics: performance and limits of ozonation and adsorption. Int J Environ Sci Technol 17:3651–3662. https://doi.org/10.1007/s13762-020-02711-2

Gümüş D, Akbal F (2017) A comparative study of ozonation, iron coated zeolite catalyzed ozonation and granular activated carbon catalyzed ozonation of humic acid. Chemosphere 174:218–231. https://doi.org/10.1016/j.chemosphere.2017.01.106

Guo S, Luo J, Yang Q, Qiang X, Feng S, Wan Y (2019) Decoloration of molasses by ultrafiltration and nanofiltration: unraveling the mechanisms of high sucrose retention. Food Bioprocess Technol 12:39–53. https://doi.org/10.1007/s11947-018-2189-z

Hoarau J, Caro Y, Grondin I, Petit T (2018) Sugarcane vinasse processing: toward a status shift from waste to valuable resource. A review. J Water Process Eng 24:11–25. https://doi.org/10.1016/j.jwpe.2018.05.003

Hollman J, Khan MF, Dominic JA, Achari G (2020) Pilot-scale treatment of neutral pharmaceuticals in municipal wastewater using reverse osmosis and ozonation. J Environ Eng 146(11):04020121. https://doi.org/10.1061/(ASCE)EE.1943-7870.0001777

Janknecht P, Wilderer PA, Picard C, Larbot A (2001) Ozone–water contacting by ceramic membranes. Sep Purif Technol 25(1–3):341–346. https://doi.org/10.1016/s1383-5866(01)00061-2

Kaushik A, Basu S, Batra VS, Balakrishnan M (2018) Fractionation of sugarcane molasses distillery wastewater and evaluation of antioxidant and antimicrobial characteristics. Ind Crops Prod 118:73–80. https://doi.org/10.1016/j.indcrop.2018.03.040

Korniłłowicz-Kowalska T, Rybczyńska-Tkaczyk K (2021) Decolorization and biodegradation of melanoidin contained in beet molasses by an anamorphic strain of *Bjerkandera adusta* CCBAS930 and its mutants. World J Microbiol Biotechnol 37:1. https://doi.org/10.1007/s11274-020-02944-w

Kotsiopoulou NG, Liakos TI, Lazaridis NK (2016) Melanoidin chromophores and betaine osmoprotectant separation from aqueous solutions. J Mol Liq 216:496–502. https://doi.org/10.1016/j.molliq.2016.01.063

Li Y, Yi R, Yan A, Deng L, Zhou K, Liu X (2009) Facile synthesis and properties of $ZnFe_2O_4$ and $ZnFe_2O_4$/polypyrrole core-shell nanoparticles. Solid State Sci 11:1319–1324. https://doi.org/10.1016/j.solidstatesciences.2009.04.014

Li L, Yuan Z, Sun Y, Kong X, Dong P, Zhang J (2017) A reused method for molasses-processed wastewater: effect on silage quality and anaerobic digestion performance of *Pennisetum purpereum*. Biores Technol 241:1003–1011. https://doi.org/10.1016/j.biortech.2017.04.117

Li W, Yu-Yu E, Cheng LY, Ding M, Li WY, Diao KS, Jiang JX (2020) Rosin-based polymer@silica core–shell adsorbent: preparation, characterization, and application to melanoidin adsorption. LWT 132:109937. https://doi.org/10.1016/j.lwt.2020.109937

Liang Z, Wang Y, Zhou Y, Liu H, Wu Z (2009) Variables affecting melanoidins removal from molasses wastewater by coagulation/flocculation. Sep Purif Technol 68(3):382–389. https://doi.org/10.1016/j.seppur.2009.06.011

Liu ZQ, Ma J, Cui YH, Zhang BP (2009) Effect of ozonation pretreatment on the surface properties and catalytic activity of multi-walled carbon nanotube. Appl Catal B 92(3–4):301–306. https://doi.org/10.1016/j.apcatb.2009.08.007

Luciano AJR, Soletti LS, Ferreira MEC, Cusioli LF, de Andrade MB, Bergamasco R, Yamaguchi NU (2020) Manganese ferrite dispersed over graphene sand composite for methylene blue photocatalytic degradation. J Environ Chem Eng 8(5):104191. https://doi.org/10.1016/j.jece.2020.104191

Mabuza J, Otieno B, Apollo S, Matshediso B, Ochieng A (2017) Investigating the synergy of integrated anaerobic digestion and photodegradation using hybrid photocatalyst for molasses wastewater treatment. Euro-Mediterr J Environ Integr 2:17. https://doi.org/10.1007/s41207-017-0029-6

Machado PR, Soeira TVR, Pagan FS, Malpass GRP, Gonçalves JCSI, Ferreira DC (2020) Synergistic bromothymol blue dye degradation with hydrodynamic cavitation and hydrogen peroxide (HC-H_2O_2). Revista Ambiente e Agua. https://doi.org/10.4136/ambi-agua.2518

Machuno LGB, Oliveira AR, Furlan RH, Lima AB, Morais LC, Gelamo RV (2015) Multilayer graphene films obtained by dip coating technique. Mater Res 18(4):775–780. https://doi.org/10.1590/1516-1439.005415

Malik SN, Ghosh PC, Vaidya AN, Mudliar SN (2019) Ozone pre-treatment of molasses-based biomethanated distillery wastewater for enhanced bio-composting. J Environ Manag 246:42–50. https://doi.org/10.1016/j.jenvman.2019.05.087

Marimón-Bolívar W, González EE (2018) Study of agglomeration and magnetic sedimentation of glutathione@Fe_3O_4 nanoparticles in water medium. DYNA 85(205):19–26. https://doi.org/10.15446/dyna.v85n205.68245

Mohsin GF, Schmitt FJ, Kanzler C, Epping JD, Buhrke D, Hornemann A (2020) Melanoidin formed from fructosylalanine contains more alanine than melanoidin formed from d-glucose with L-alanine. Food Chem 305:125459. https://doi.org/10.1016/j.foodchem.2019.125459

Momeni MM, Kahforoushan D, Abbasi F, Ghanbarian S (2018) Using chitosan/CHPATC as coagulant to remove color and turbidity of industrial wastewater: optimization through RSM design. J Environ Manag 211:347–355. https://doi.org/10.1016/j.jenvman.2018.01.031

Natividade PSG, de Moraes MG, Avallone E, Bandarra FEP, Gelamo RV, Gonçalves JCSI (2019) Experimental analysis applied to an evacuated tube solar collector equipped with parabolic concentrator using multilayer graphene-based nanofluids. Renew Energy 138:152–160. https://doi.org/10.1016/j.renene.2019.01.091

Nawrocki J (2013) Catalytic ozonation in water: controversies and questions. Discussion paper. Appl Catal B Environ 142–143:465–471. https://doi.org/10.1016/j.apcatb.2013.05.061

Nawrocki J, Kasprzyk-Hordern B (2010) The efficiency and mechanisms of catalytic ozonation. Appl Catal B 99(1–2):27–42. https://doi.org/10.1016/j.apcatb.2010.06.033

Nečas D, Klapetek P, Gwyddion P (2012) An open-source software for SPM data analysis. Cent Eur J Phys 10(1):181–188. https://doi.org/10.2478/s11534-011-0096-2

Nguyen DMT, Bartley JP, Doherty WOS (2017) Combined fenton oxidation and chemical coagulation for the treatment of melanoidin/phenolic acid mixtures and sugar juice. Ind Eng Chem Res 56(6):1385–1393. https://doi.org/10.1021/acs.iecr.6b04001

Oliveira JSD, Salla JDS, Kuhn RC, Jahn SL, Foletto EL (2019) Catalytic ozonation of melanoidin in aqueous solution over $CoFe_2O_4$ catalyst. Mater Res. https://doi.org/10.1590/1980-5373-mr-2018-0405

Omar AA, Mahgoub S, Salama A, Likotrafiti E, Rhoades J, Christakis C, Samaras P (2020) Evaluation of *Lactobacillus kefiri* and manganese peroxidase producing-bacteria for decolorization of melanoidins and reduction of chemical oxygen demand. Water Environ J. https://doi.org/10.1111/wej.12663

Otieno B, Apollo S (2021) Energy recovery from biomethanation of vinasse and its potential application in ozonation post-treatment for removal of biorecalcitrant organic compounds. J Water Process Eng 39:101723. https://doi.org/10.1016/j.jwpe.2020.101723

Otieno B, Apollo S, Naidoo B, Ochieng A (2019) Modeling ozonation pretreatment parameters of distillery wastewater for improved biodegradability. J Environ Sci Health Part A 54(11):1066–1074. https://doi.org/10.1080/10934529.2019.1631089

Peña M, Coca M, Gonzalez G, Rioja R, Garcia MT (2003) Chemical oxidation of wastewater from mollasses fermentation with ozone. Chemosphere 51(9):893–900. https://doi.org/10.1016/S0045-6535(03)00159-0

Pereira JFS, Borges PHS, Moura GM, Gelamo RV, Nossol E, Canobre SC, Munoz RAA (2019) Improved electrochemical performance of pyrolytic graphite paper: electrochemical versus reactive cold-plasma activation. Electrochem Commun 105:106497. https://doi.org/10.1016/j.elecom.2019.106497

Poblete R, Cortes E, Salihoglu G, Salihoglu NK (2020) Ultrasound and heterogeneous photocatalysis for the treatment of vinasse from pisco production. Ultrason Sonochem 61:104825. https://doi.org/10.1016/j.ultsonch.2019.104825

Rafigh SM, Soleymani AR (2020) Melanoidin removal from molasses wastewater using graphene oxide nanosheets. Sep Sci Technol 55(13):2281–2293. https://doi.org/10.1080/01496395.2019.1626424

Raji M, Mirbagheri SA, Ye F, Dutta J (2021) Nano zero-valent iron on activated carbon cloth support as Fenton-like catalyst for efficient color and COD removal from melanoidin wastewater. Chemosphere 263:127945. https://doi.org/10.1016/j.chemosphere.2020.127945

Ripper B, Kaiser CR, Perrone D (2020) Use of NMR techniques to investigate the changes on the chemical composition of coffee melanoidins. J Food Compos Anal 87:103399. https://doi.org/10.1016/j.jfca.2019.103399

Rizvi S, Goswami L, Gupta SK (2020) A holistic approach for melanoidin removal via Fe-impregnated activated carbon prepared from *Mangifera indica* leaves biomass. Bioresour Technol Rep 12:100591. https://doi.org/10.1016/j.biteb.2020.100591

Romero P, Coello MD, Aragón CA, Battistoni P, Eusebi AL (2015) Sludge reduction through ozonation: effects of different specific dosages and operative management aspects in a full-scale study. J Environ Eng 141(12):04015043. https://doi.org/10.1061/(asce)ee.1943-7870.0001006

Sachs S, Bernhard G (2011) Influence of humic acids on the actinide migration in the environment: suitable humic acid model substances and their application in studies with uranium—a review. J Radioanal Nucl Chem 290:17–29. https://doi.org/10.1007/s10967-011-1084-0

Satori H, Kawase Y (2014) Decolorization of dark brown colored coffee effluent using zinc oxide particles: the role of dissolved oxygen in degradation of colored compounds. J Environ Manag 139:172–179. https://doi.org/10.1016/j.jenvman.2014.02.032

Setareh P, Khezri SM, Hossaini H, Pirsaheb M (2020) Coupling effect of ozone/ultrasound with coagulation for improving NOM

and turbidity removal from surface water. J Water Process Eng 37:101340. https://doi.org/10.1016/j.jwpe.2020.101340

Silva GA, Ferreira SL, de Souza GR, da Silva JA, Pagliuso JD (2019) Utilization of a new approach for the potassium concentration of sugarcane vinasse by reverse osmosis: case study. Int J Environ Sci Technol 16:6441–6446. https://doi.org/10.1007/s13762-019-02209-6

Singh N, Petrinic I, Hélix-Nielsen C, Basu S, Balakrishnan M (2018) Concentrating molasses distillery wastewater using biomimetic forward osmosis (FO) membranes. Water Res 130:271–280. https://doi.org/10.1016/j.watres.2017.12.006

Takashina TA, Leifeld V, Zelinski DW, Mafra MR, Igarashi-Mafra L (2017) Application of response surface methodology for coffee effluent treatment by ozone and combined ozone/UV. Ozone Sci Eng 40(4):293–304. https://doi.org/10.1080/01919512.2017.1417112

Talaiekhozani A, Rezania S (2017) Application of photosynthetic bacteria for removal of heavy metals, macro-pollutants and dye from wastewater: a review. J Water Process Eng 19:312–321. https://doi.org/10.1016/j.jwpe.2017.09.004

Tao H, Moser J, Alzina F, Wang Q, Sotomayor-Torres CM (2011) The morphology of graphene sheets treated in an ozone generator. J Phys Chem C 115(37):18257–18260. https://doi.org/10.1021/jp2050756

Thanapimmetha A, Srinophakun P, Amat S, Saisriyoot M (2017) Decolorization of molasses-based distillery wastewater by means of pulse electro-Fenton process. J Environ Chem Eng 5(3):2305–2312. https://doi.org/10.1016/j.jece.2017.04.030

Toomsan W, Mungkarndee P, Boonlue S, Giao NT, Siripattanakul-Ratpukdi S (2020) Potential degradation and kinetics of melanoidin by using laccase from white rot fungus. Appl Environ Res 42(3):1–10. https://doi.org/10.35762/AER.2020.42.3.1

Tripathy BK, Johnson I, Kumar M (2020) Melanoidin removal in multi-oxidant supplemented microwave system: optimization of operating conditions using response surface methodology and cost estimation. J Water Process Eng 33:101008. https://doi.org/10.1016/j.jwpe.2019.101008

Tsiakiri EP, Sompatzi E, Voukia MP, Sotiropoulos S, Pantazaki AA (2020) Biocatalytic and bioelectrolytic decolorization of simulated melanoidin wastewaters by *Saccharomyces cerevisiae* cells suspended and conjugated on silica and alumina. J Environ Chem Eng 8(5):104078. https://doi.org/10.1016/j.jece.2020.104078

Tsioptsias C, Lionta G, Samaras P (2016) Microalgae-activated sludge treatment of molasses wastewater in sequencing batch photo-bioreactor. Environ Technol 38(9):1120–1126. https://doi.org/10.1080/09593330.2016.1218552

Vivekanandam S, Muthunarayanan V, Muniraj S, Rhyman L, Alswaidan IA, Ramasami P (2019) Ingenious bioorganic adsorbents for the removal of distillery based pigment-melanoidin: preparation and adsorption mechanism. J Macromol Sci Part A 56(1):52–62. https://doi.org/10.1080/10601325.2018.1527180

Wang Y, Xie Y, Sun H, Xiao J, Cao H, Wang S (2016) Efficient catalytic ozonation over reduced graphene oxide for *p*-hydroxylbenzoic acid (PHBA) destruction: active site and mechanism. ACS Appl Mater Interfaces 8(15):9710–9720. https://doi.org/10.1021/acsami.6b01175

Wang Z, Mab H, Zhang C, Feng J, Pu S, Rend Y, Wang Y (2018) Enhanced catalytic ozonation treatment of dibutyl phthalate enabled by porous magnetic Ag-doped ferrospinel $MnFe_2O_4$ materials: performance and mechanism. Chem Eng J 354:42–52. https://doi.org/10.1016/j.cej.2018.07.177

Wei K, Cao X, Gu W, Liang P, Huang X, Zhang X (2019) Ni-induced C-Al_2O_3-framework (NiCAF) supported core-multishell catalysts for efficient catalytic ozonation: a structure-to-performance study. Environ Sci Technol. https://doi.org/10.1021/acs.est.8b07132

Wongcharee S, Aravinthan V (2020) Application of mesoporous magnetic nanosorbent developed from macadamia nut shell residues for the removal of recalcitrant melanoidin and its fractions. Sep Sci Technol 55(9):1636–1649. https://doi.org/10.1080/01496395.2019.1606015

Xing L, Xie Y, Minakata D, Cao H, Xiao J, Zhang Y, Crittenden JC (2014) Activated carbon enhanced ozonation of oxalate attributed to HO oxidation in bulk solution and surface oxidation: effect of activated carbon dosage and pH. J Environ Sci 26(10):2095–2105. https://doi.org/10.1016/j.jes.2014.08.009

Yang F, Zhao M, Wang Z, Ji H, Zheng B, Xiao D, Guo Y (2014) The role of ozone in the ozonation process of graphene oxide: oxidation or decomposition? RSC Adv 4:58325–58328. https://doi.org/10.1039/c4ra08750j

Yuan Y, Xing G, Garg S, Ma J, Kong X, Dai P, Waite TD (2020) Mechanistic insights into the catalytic ozonation process using iron oxide-impregnated activated carbon. Water Res 177:115785. https://doi.org/10.1016/j.watres.2020.115785

Zhang Y, Li H, Huang H, Zhang Q, Guo Q (2018) Graphene oxide–supported cobalt phthalocyanine as heterogeneous catalyst to activate peroxymonosulfate for efficient degradation of norfloxacin antibiotics. J Environ Eng 144(7):04018052. https://doi.org/10.1061/(ASCE)EE.1943-7870.0001395

Zhang Z, Li D, Zhang X (2019) Enzymatic decolorization of melanoidins from molasses wastewater by immobilized keratinase. Biores Technol 280:165–172. https://doi.org/10.1016/j.biortech.2019.02.049

Zhao J, Cao J, Zhao Y, Zhang T, Zheng D, Li C (2020) Catalytic ozonation treatment of papermaking wastewater by Ag-doped $NiFe_2O_4$: performance and mechanism. J Environ Sci 97:75–84. https://doi.org/10.1016/j.jes.2020.04.014

Zhu L, Shi Z, Deng L, Duan Y (2020) Efficient degradation of sulfadiazine using magnetically recoverable $MnFe_2O_4$/δ-MnO_2 hybrid as a heterogeneous catalyst of peroxymonosulfate. Colloids Surf A 609:125637. https://doi.org/10.1016/j.colsurfa.2020.125637